



Research article

Diagnostic, prognostic, and immunological roles of CDSN in ovarian cancer

Huan Zeng^{b,1}, Wei Pan^{c,1}, Qiuyi Xia^a, Hong Shu^{b,**}, Zhaodong Ji^{a,*}

^a Department of Clinical Laboratory, Huashan Hospital, Fudan University, Shanghai, 200040, China

^b Department of Clinical Laboratory, Guangxi Medical University Cancer Hospital, Nanning, 530021, China

^c Lab for Noncoding RNA & Cancer, School of Life Sciences, Shanghai University, Shanghai, 200444, China

ARTICLE INFO

Keywords:

Ovarian cancer
Mutation
Tumor microenvironment
immunotherapy
CDSN

ABSTRACT

Globally, ovarian cancer (OC) ranks as a principal cause of cancer-related mortality in females. Immunotherapy has revolutionized the treatment of OC, but the efficacy of immunotherapy is often limited by different immune microenvironments. The objective of this research was to pinpoint and validate candidate genes with potential value as diagnostic and prognostic biomarkers and therapeutic targets in OC. Data on genes associated with gene mutation, prognostic survival, and immune infiltration in OC were procured from the Cancer Genome Atlas (TCGA). Gene differential analysis, mutation site analysis, prognosis and survival analysis, and functional and signaling pathway enrichment analysis were conducted to identify and evaluate key genes. The genes were further investigated using immune infiltration analysis, receiver operating characteristic curves, and immunohistochemistry. The impact of *CDSN* on OC cell proliferation was investigated utilizing CCK-8, colony formation, and apoptosis detection assays. We identified a set of genes (*CDSN*, *WARS*, and *CD38*) that were highly expressed in OC and significantly associated with mutations and prognosis. Immune infiltration analysis and immunohistochemistry results indicated a correlation with immune infiltration in the tumor microenvironment, particularly in antigen-presenting cells. Receiver operating characteristic curve analysis demonstrated the diagnostic potential of these three genes in OC, with all three genes showing the area under the curve (AUC) above 0.8. In vitro studies suggested that knocked down *CDSN* expression resulted in a marked lower in the proliferative capacity of OC cells. The candidate gene *CDSN* identified through bioinformatics analysis and in vitro experiments is associated with mutation and immune infiltration, showing promise as a diagnostic and prognostic biomarker, as well as a therapeutic objective in OC.

1. Introduction

Globally, ovarian cancer (OC) ranks as the eighth most prevalent malignancy among females, with an estimated 313,000 novel diagnoses and 207,000 fatalities recorded in 2020 [1]. Despite improvements in surgical concepts and techniques, as well as advances in genetic profiling, the prognosis for OC patients remains poor. Moreover, over 70 % of cases are detected in later stages, resulting in

* Corresponding author.

** Corresponding author.

E-mail addresses: shuhong@gxmu.edu.cn (H. Shu), zdji18@fudan.edu.cn (Z. Ji).

¹ These authors contributed equally to this work.

five-year survival rates below 50 % [2]. Therefore, early diagnosis and treatment are crucial for enhancing the survival outcomes of individuals with OC.

The identification of genetic susceptibility genes provides opportunities for the early detection and prevention of ovarian tumors. Previous studies show that the most significant genetic risk factors for hereditary ovarian cancer are specific alleles found in the BRCA1 and BRCA2 genes [3]. The life-time risk of OC is estimated to be 35%–70 % for women with BRCA1 mutations and 10%–30 % for women with BRCA2 mutations; by comparison, the lifetime risk of OC is less than 2 % for women in the general population [4]. Many other mutated genes play important roles in OC, including RAD51C and RAD51D, OC susceptibility genes associated with hereditary OC [5], and BRIP1, in which deleterious germline mutations are associated with hereditary OC [6]. Further identification of mutated genes associated with OC is expected to contribute to future advances in OC screening and diagnosis.

Prior research has suggested that the progression of OC is not only linked to tumor cells, but it is also closely connected to the tumor microenvironment [7]. The interaction between the tumor microenvironment and tumor cells has an important impact on prognosis and treatment outcome [8]. The OC tumor microenvironment consists of immune cell populations in the tumor, peripheral blood, and ascites and includes T and B lymphoid cells, tumor-associated macrophages, natural killer cells, platelets, and dendritic cells. These cells play a role in the response to immunotherapy in individuals with OC [9–11].

In this study, our objective was to identify potential biomarkers and therapeutic targets for OC by conducting a comprehensive analysis of genes that are significantly associated with mutation, prognosis, and the tumor microenvironment.

2. Materials and methodologies

2.1. Data source and preprocessing

RNA-seq data for OC tissues and normal ovarian tissues were obtained from UCSC Xena (<http://xena.ucsc.edu>). Within this platform, data from 427 OC cases were from the Cancer Genome Atlas (TCGA)-OV cohort and data from 88 normal ovaries were from Genotype-tissue expression (GTEx): The data were preprocessed as follows: log2 transformation ($\log_2(\text{norm_count} + 1)$) of RNA-seq expression dataset was downloaded, and gene copy number variations (CNVs) and mutation data from the TCGA-OV cohort and related clinical phenotype data were obtained.

2.2. Identification of differentially expressed genes (DEGs) and chromosomal localization

The R package limma was employed to detect and extract the DEGs in OC, using a false discovery rate (FDR) < 0.05 and a log fold change (FC) > 1. The chromosomal location distribution of these differential genes was visualized using the Gene Expression Profiling Interactive Analysis (GEPIA) tool.

2.3. Gene mutation analysis

Mutation data from the TCGA-OV cohort were analyzed using the maftools package. The cBioportal database (<https://www.cbioportal.org/>) integrates multiple data from TCGA and is used to study the statistics of genomic alterations in tumor samples. Overexpressed genes overlapping with mutated genes were included as candidates in the subsequent analyses.

2.4. Functional and pathway enrichment analysis

The enrichment analysis of candidate genes was carried out utilizing the cluster Profiler package in R. For instance, Gene Ontology (GO), Kyoto Encyclopedia of Genes and Genomes (KEGG) pathway, HALLMARK, and REACTOME analyses. $P < 0.05$ suggested significant enrichment. Genes enriched in cellular component (CC), biological process (BP), molecular function (MF) terms, metabolic pathway, and signal transduction pathways were identified.

2.5. Identification of potential prognostic genes

Cox univariate regression analysis was performed on TCGA data utilizing the R package “survival” (v3.2-7) and “survminer” (v0.4.8) in conjunction with overall survival (OS) and progression-free survival (PFS) data. A value of $p < 0.05$ was established to identify genes with potential prognostic significance. The overlapping genes in the overexpressed and mutated gene sets were intersected with the candidate genes to identify potential prognostic genes. The optimal grouping threshold for the relevant genes was determined utilizing the surv_cutpoint function from the “survminer” R software package. The surv_cutpoint function calculates Maximally Selected Rank Statistics based on the maxstat.test function of the “maxstat” package to determine the best threshold by maximizing the difference. The data were grouped using this threshold, and Kaplan–Meier curves were constructed for survival data analysis. The survival package was employed to perform the log-rank test for comparison between groups.

2.6. Immune infiltration analysis and immune subtype correlation analysis

The Tumor Immune Estimation Resource (TIMER) online database <https://cistromeshinyapps.io/timer/> was employed to identify relationships between potential prognostic genes and B cells, CD4⁺T cells, CD8⁺T cells, neutrophils, macrophages, and dendritic cells.

The 'subtype' module of the TISIDB database (<http://cis.Hku.hk/TISIDB/>) was employed to investigate the associations among the expression of potential genes and molecular or immune subtypes in OC. The TISIDB database integrates diverse data types for assessing the interaction between cancer and the immune system, providing a comprehensive description of this relationship.

2.7. Immunohistochemistry analysis

Ovarian tissues were collected from two individuals receiving treatment at Huashan Hospital of Fudan University. One case was pathologically diagnosed as serous ovarian cancer, and the other was normal ovarian tissue (oviduct). This research received ethical clearance from the Ethics Committee of Huashan Hospital, Fudan University (code KY2022-642). All participants signed informed consent forms for clinical research.

Normal ovarian and ovarian cancer tissues were treated with 10 % formalin and subsequently embedded in paraffin. The paraffin blocks were sectioned into 5 mm slices, deparaffinized with xylene, and hydrated with gradient ethanol. Microwave heating with 10 mM sodium citrate buffer (pH 6.0) at 95 °C was employed for antigen retrieval. The activity of endogenous peroxidase was quenched using 3 % H₂O₂ at ambient temperature. Slices were treated with 3 % bovine serum albumin (BSA) at room temperature to prevent non-specific binding. The tissue slices were treated with the primary antibody anti-WARS (dilution 1:100; #16081-1-AP, Proteintech, China), anti-CDSN (dilution 1:100; #13184-1-AP, Proteintech), anti-CD38 (dilution 1:100; #25284-1-AP, Proteintech), anti-CD20 (dilution 1:100; #24828-1-AP, Proteintech), anti-CD11c (dilution 1:100; #17342-1-AP, Proteintech) and anti-CD68 (dilution 1:100; #28058-1-AP, Proteintech). Slices were then rinsed in phosphate buffered saline (PBS) and treated with anti-rabbit secondary antibody at ambient temperature. Secondary antibodies against rabbit IgG were procured from the IHC EnVision™ Detection kit (GENE, USA). Slices were stained with diaminobenzidine and hematoxylin. Finally, slices were subjected to ethanol dehydration, xylene clearing, and subsequently covered with a coverslip. Five different fields were randomly selected to assess protein expression levels by microscopy.

The Image J analysis software (1.51K, USA) was used to quantify the cumulative optical density (IOD) and corresponding positive pixel area in each slice, with pixel area serving as the standard unit. The mean optical density (MOD) was calculated by dividing the cumulative optical density by the positive pixel area.

2.8. Cell culture and transfection

OC cell lines HEY and SKOV3 were procured from the American Type Culture Collection (ATCC) and maintained in Roswell Park Memorial Institute 1640 medium (Solarbio) or DMEM (Solarbio) enriched with 10 % fetal bovine serum. Cells were grown in a moisture-controlled incubator at 37 °C with 5 % CO₂.

Three distinct small interfering RNAs (siRNAs) designed to suppress *CDSN* expression and a negative control siRNA were procured from RiboBio Company (Shanghai, China). OC cells were transfected using Lipofectamine 3000 (Invitrogen, Grand Island, NY, USA) for 48 h and then collected for further analysis.

2.9. RNA extraction and qRT-PCR analysis

Total RNA was isolated from approximately 1–2 × 10⁶ cells utilizing TRIzol reagent (Invitrogen, CA, USA). The primer sequences utilized in this study were: *CDSN*, forward: TCTCAGACCCCTGTAAGGACC and reverse: CGTTCCTGGCTTAAAAGATCCTG; *GAPDH*, forward: GGAGCGAGATCCCTCCAAAAT and reverse: GGCTGTTGTCATACTTCTCATGG. The reaction conditions were 95 °C for 30 s and 95 °C for 5 s, and 60 °C for 30 s for 45 amplification cycles.

2.10. Cell counting Kit-8 assay

Cell proliferation was evaluated utilizing the Cell Counting Kit-8 (CCK-8) kit. Cells in the logarithmic phase were plated in a 96-well culture plate (Corning, NY, USA) at 3–5 × 10³ per well with 100 μL of medium per well. Following incubation periods of 24, 48, 72, and 96 h, 10 μL of CCK-8 was introduced, and cells were subsequently incubated at 37 °C for 1 h. The absorbance was measured at 450 nm utilizing a microplate reader (Thermo, MA, USA) to identify the optical density value. The experiment was done in triplicate.

2.11. Colony formation assay

Logarithmically growing cells were plated in 6-well plates (SKOV3: 2000 cells/well, HEY: 1000 cells/well, OVCA433: 2000 cells/well) and incubated at 37 °C. After 10 days, the cultures were terminated. The cells were rinsed with PBS and fixed utilizing methanol for 15 min at ambient temperature. After discarding the methanol, the cells were washed and stained with crystal violet solution (0.1 %) for 10 min before being air-dried. Colonies containing more than 50 cells were quantified.

2.12. Western blotting

The OC cells were seeded in 6-well plates and transfected with siRNAs as described above. Following 48 h of incubation, cells were lysed in RIPA lysis buffer. Equivalent quantities of proteins were resolved on 10 % sodium dodecyl sulfate-polyacrylamide gel electrophoresis (SDS-PAGE). The protein was then electroblotted onto a PVDF membrane under constant current conditions, and the

membrane was blocked with 5 % skim milk powder for 2 h at ambient temperature to obstruct nonspecific binding sites. The membrane was mixed with anti-CDSN antibody (dilution:1:1000; #13184-1-AP, Proteintech) and GAPDH in antibody (dilution:1:1000; #60004-1-Ig, Proteintech) were incubated overnight at 4 °C. GAPDH was used as a protein loading control. After rinsing with Tris-buffered saline-Tween (TBST), the cells were incubated with HRP-labeled anti-rabbit secondary antibody (dilution:1:5000; #RGAR001, Proteintech) for 2 h at ambient temperature. Protein detection was performed utilizing an Image Lab system (Bio-Rad, Hercules, CA).

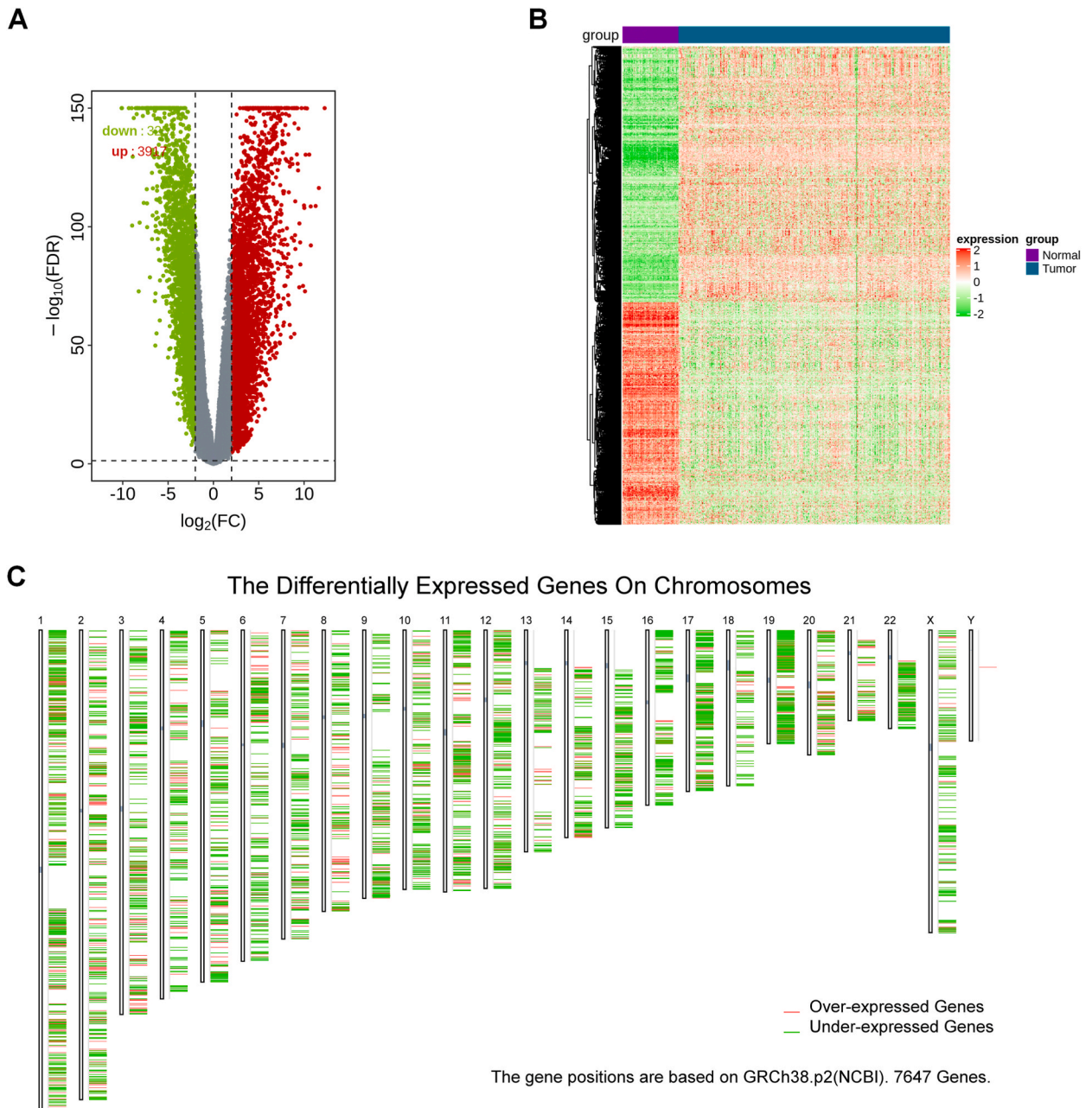


Fig. 1. Differential expressed gene (DEG) analysis on OC. (A) Volcano plots of gene expression in unpaired samples of 399 ovarian cancer and 88 normal tissues from TCGA. DEGs screened based on false discovery rate <0.05 and $|\log_2 FC| > 1$. Red color indicates degree of up-regulation, green color indicates degree of down-regulation, and grey color indicates genes without differential expression. (B) Heat map of DEGs. (C) Distribution of differential genes on chromosomes.

2.13. Analysis of cell apoptosis by flow cytometry

The OC cells were seeded in 6-well plates and transfected with siRNA targeting CDSN. Following 48 h of incubation, cells were harvested, rinsed with cold PBS, and resuspended at 1×10^6 /mL. The cells were then incubated with 5 μ L of 7AAD and Annexin V-PE (BD, USA) for 15 min under dark conditions at ambient temperature. Subsequently, the cells were examined utilizing a flow cytometer (Cytomics FC 500 MPL, Beckman Coulter, USA). Early apoptosis was indicated by the proportion of cells showing Annexin V+/7AAD-, whereas late apoptosis was assessed by the percentage of cells exhibiting Annexin V+/7AAD+. The findings presented are the mean

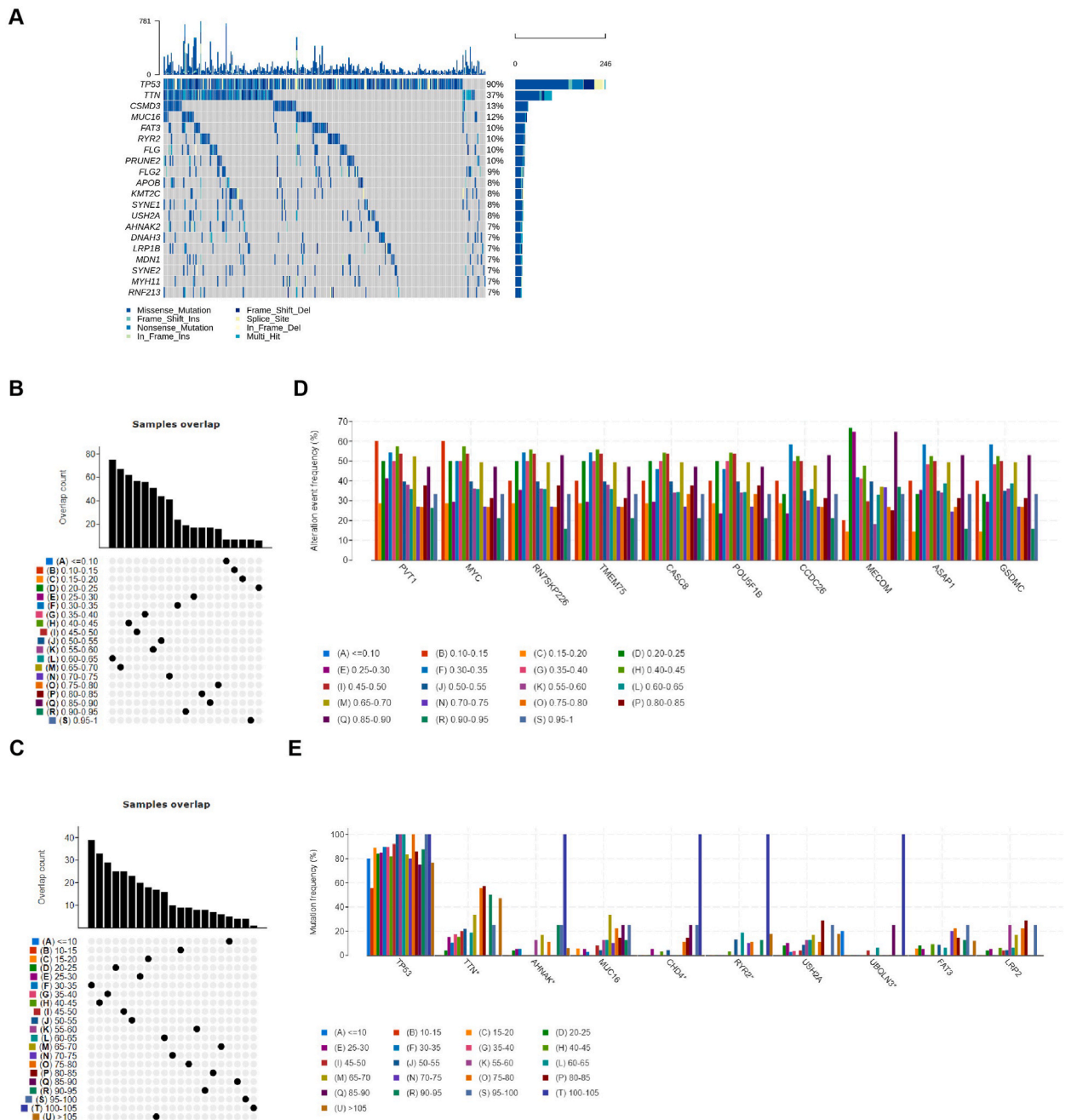


Fig. 2. Determination of gene mutation and type of mutation in OC. (A)Waterfall map of mutated genes. (B) Group statistics of the CNV change values of genes; The genes were categorized into 19 groups, labeled as A-S groups, based on the proportion of CNV variants occurring within the range of 0.1–1. (C) Group statistics of the number of mutated genes; The gene mutations divided into 21 groups, designated A-U, based on the range of numbers (10–105). (D) Distribution of genes with the top ten CNV change values in different groups. (E) Distribution of genes with the top ten mutation numbers in different groups.

values obtained from three independent determinations.

2.14. Statistical analysis

Statistical analysis was performed utilizing R software. The prognostic value of the genes was evaluated via Cox univariate analysis. Kaplan–Meier curves were employed to evaluate survival, and the log-rank test was utilized to identify the statistical significance of differences in the curves. The utility of genetic testing in diagnosis was assessed with ROC curves. We conducted a correlational study

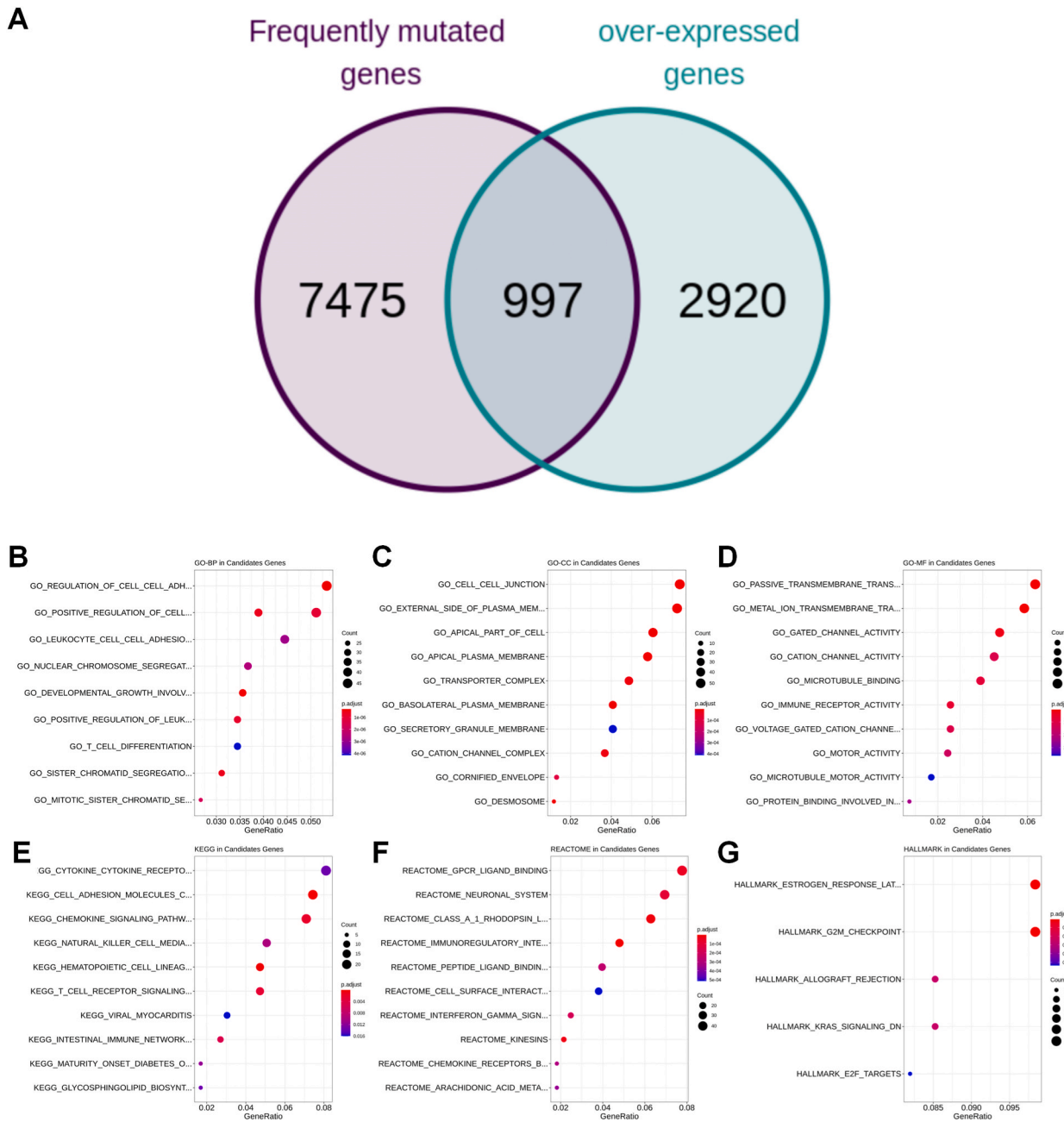


Fig. 3. Functional and signaling pathway enrichment analysis of candidate genes. (A) Venn diagram of the intersection of overexpressed genes and mutated genes. The top 10 significantly enriched entries for GO-BP (B), GO-CC (C), and GO-MF (D) enrichment analysis of candidate differential genes. The top 10 significantly enriched pathways for KEGG (E), HALLMARK (F), and REACTOME (G) enrichment analysis of candidate differential genes. The size of the dots is proportional to the number of genes, and the color of the dots is related to the p-value. The color of the dots indicates the significance level of the enrichment entry or pathway.

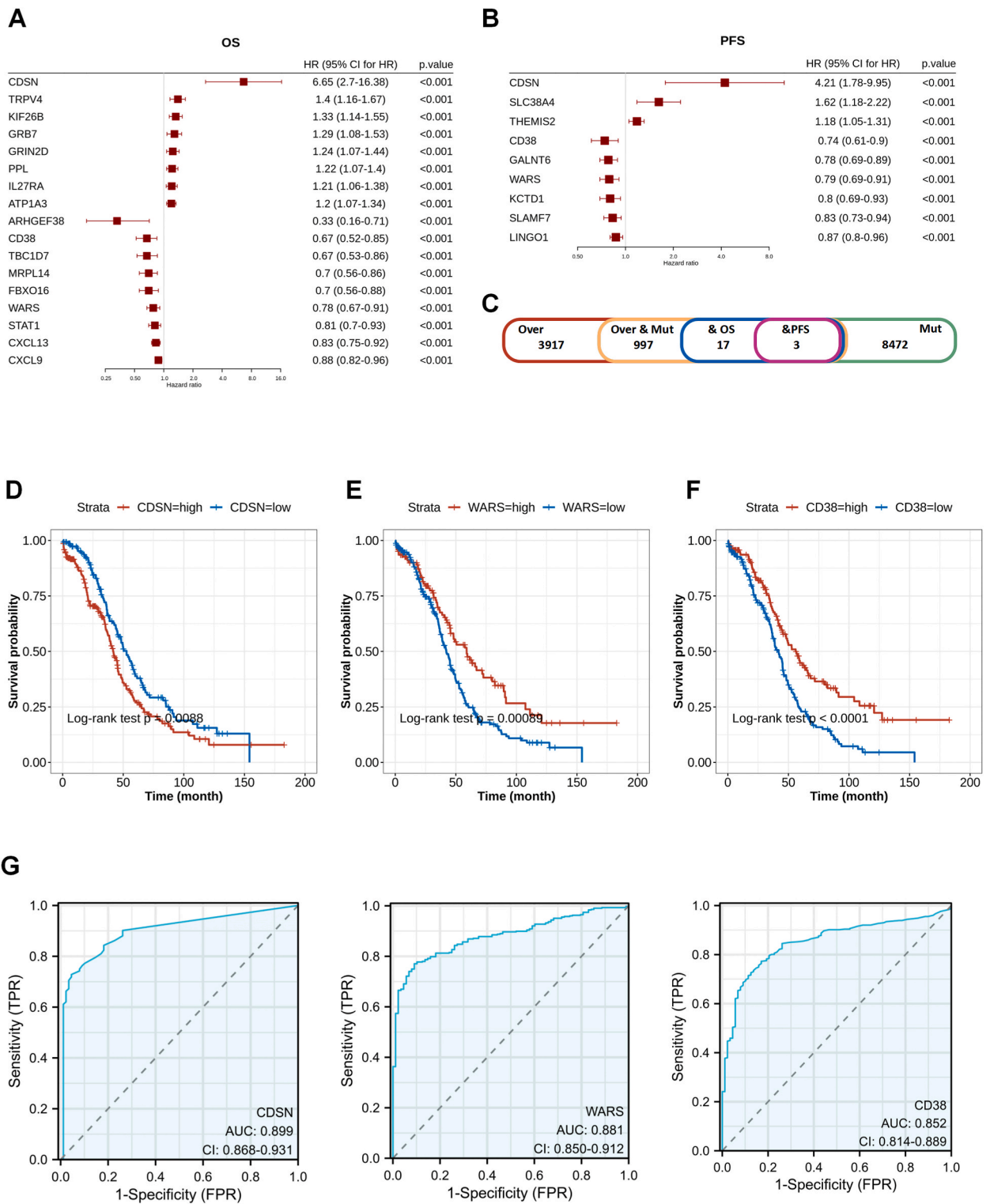


Fig. 4. Identification and verification of prognostic potential genes in OC. (A) Forest plot of prognostic-related genes screened based on one-factor cox risk proportion regression for OS. (B) Forest plot of prognostic-related genes screened based on one-factor cox risk proportion regression for PFS. (C) Candidate genes with both high expression and mutation (997), of which three were significantly correlated with OS and PFS. (D–F) Prognostic analyses of ovarian cancer patients based on *CDSN*, *WARS*, *CD38* mRNA levels calculated by the Kaplan–Meier survival curves. (G) Analysis of the clinical diagnostic performance of candidate genes by ROC curves.

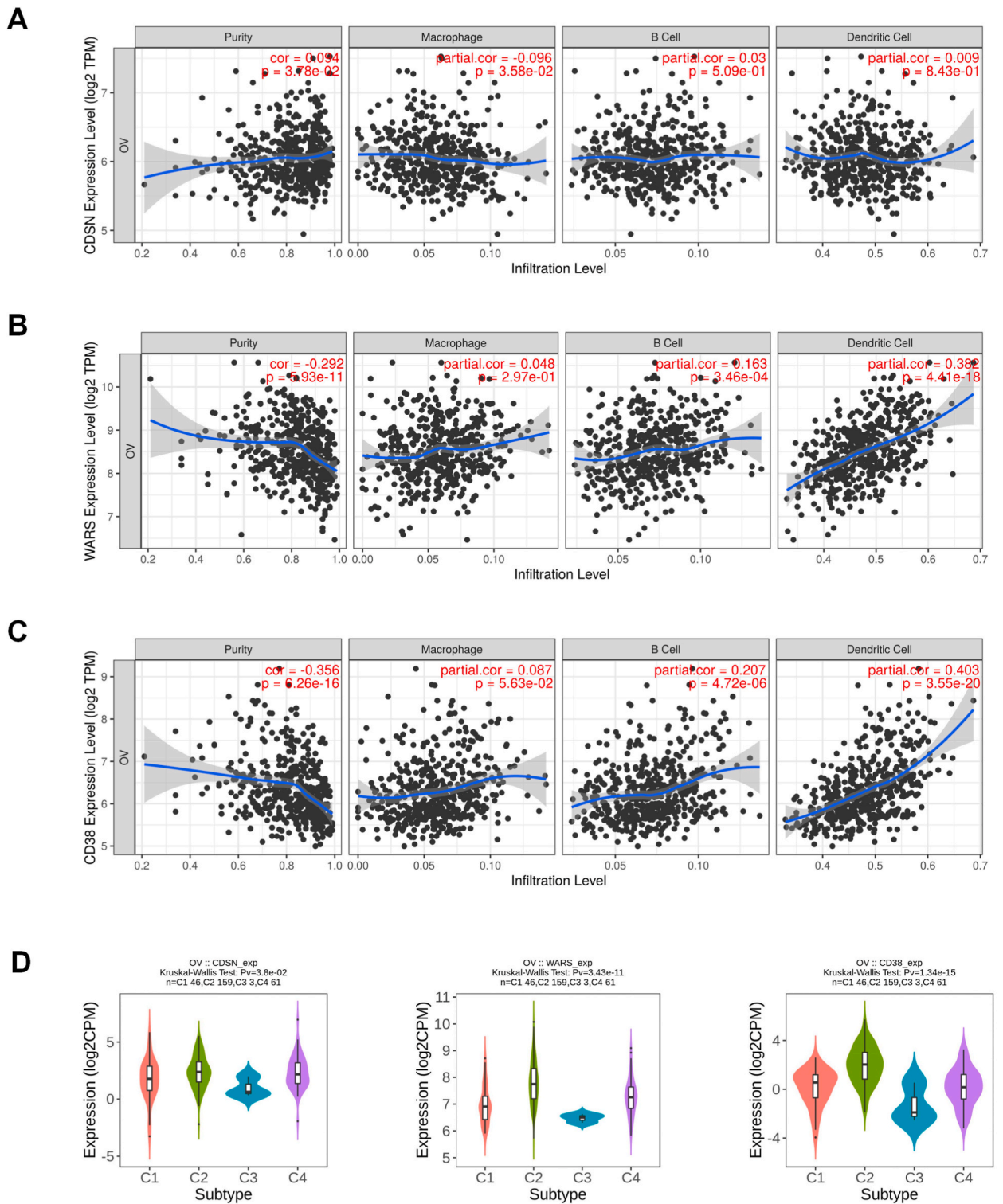


Fig. 5. Correlation and diagnostic value of candidate genes with immune cells. Correlation of (A) CDSN, (B) WARS, and (C) CD38 with B cells, macrophages, and dendritic cells. (D) Correlation between expression of candidate genes and tumor immune subtypes. C1 (wound healing), C2 (IFN-1 dominant), C3 (inflammatory), C4 (lymphocyte deplete).

of candidate genes with immune cells and subtypes. Data were analyzed by GraphPad Prism 9.5 and are denoted as mean \pm standard deviation. The *t*-test was employed to compare the two groups. Statistically significant differences between the various groups were identified utilizing a one-way analysis of variance, setting the significance threshold at $P < 0.05$.

3. Results

3.1. Identification of DEGs in OC

We searched the transcriptome expression profile data of the TCGA-OV cohort and the transcriptome data of normal ovarian tissues from UCSC Xena, including 88 tumor-free samples and 427 OC samples (28 transcriptome-free data samples were filtered). DEGs were identified utilizing the criteria of $FDR < 0.05$ and $|\log_2 FC| > 1$, which revealed 3917 upregulated genes and 3252 downregulated genes (Fig. 1A and B). GEPIA was used to map the positional distribution of DEGs on chromosomes (Fig. 1C).

3.2. Determination of gene mutation and type of mutation in OC

Analysis of data of mutated genes from the TCGA-OV tissue cohort (Fig. 2A) was used to investigate genomic alterations in tumor samples, including the fraction of CNVs and variant genes (fraction of genome altered) in individual samples (Fig. 2B and D) and tumor gene mutation counts (Fig. 2C and E). A total of 997 candidate genes were obtained by intersection of frequently mutated genes and over-expressed genes (Fig. 3A).

3.3. Functional and signaling pathway enrichment analysis of candidate genes

An enrichment analysis was carried out to examine the association of candidate genes with signaling pathways. Gene Ontology (GO) biological process (BP) analysis suggested that candidate genes were mainly involved in cell adhesion regulation and leukocyte adhesion, while GO cellular component (CC) analysis showed that candidate genes were primarily located in the cell junction, external side of the plasma membrane, and the apical plasma membrane. Molecular functions (MF) mainly included transmembrane transport, metal ion transmembrane transport, and gated channel activity (Fig. 3B–D). KEGG analysis suggested that the genes were mainly linked to cytokine receptors, cell adhesion, and chemokine signaling pathways (Fig. 3E).

REACTOMEK analysis suggested that candidate genes were markedly enriched in GPCR ligand binding, neuronal systems, and class A1 rhodopsin (Fig. 3F). Using HALLMARK analysis, candidate genes were found to be enriched at the late estrogen response and G2M checkpoint (Fig. 3G).

3.4. Identification and verification of prognostic potential genes in OC

Univariate regression analysis of the candidate gene batches combined with clinical outcome data revealed 17 genes significantly associated with OS and 10 genes markedly linked to progression-free survival (Fig. 4A and B). The intersection of these sets identified three candidate genes: *CDSN*, *WARS*, and *CD38*. Kaplan–Meier curve analysis suggested that elevated *CDSN* expression was linked to a less favorable outcome in OC individuals, whereas increased expression of *WARS* and *CD38* correlated with an improved prognosis (Fig. 4D–F).

The diagnostic potential of the three genes of interest was further evaluated utilizing ROC curves. As depicted in Fig. 4G, all three genes demonstrated good diagnostic value in OC, with AUC values that exceeded 0.8.

3.5. Correlation between gene expression and tumor-infiltrating immune cells

We utilized TIMER data to analyze the expression of potential prognostic genes and association with B cells, T cells, CD4⁺ and CD8⁺T cells, neutrophils, macrophages, and dendritic cells, with particular focus on the association between the potential genes and the level of infiltration of antigen-presenting cells (i.e., B cells, macrophages, and dendritic cells). Scatter plots showed that *WARS* and *CD38* were positively associated with the level of antigen-presenting cell infiltration (Fig. 5A–C). Scatter plots of the levels of other immune cell infiltrates with potential gene associations are shown in Supplementary Fig. 1. These findings suggest that the three candidate genes play a crucial role in antigen presentation during immunological reactions in OC cells.

The Cancer Immune Landscape comprises six distinct subtypes: C1 (wound healing), C2 (IFN-1), C3 (inflammatory), C4 (lymphocyte depleted), C5 (immunologically quiet), and C6 (TGF- β dominant). These subtypes are determined by the presence of macrophage or lymphocyte signatures, exhibiting immense potential for prognostic analysis and targeted therapy. We investigated the expression levels of the three genes across the immune subtypes of OC and found that the genes were differentially expressed in C1–C4 (Fig. 5D). These results suggest that the three genes may play different roles in different molecular or immune subtypes in the prognosis of OC.

3.6. Immuno-infiltration validation of the three genes by immunohistochemistry

To further verify the association between the three genes and immune infiltration, immunohistochemical analysis was performed on clinical OC tissue samples. The results showed the expression of *CD38*, *WARS*, and *CDNS* and the infiltration of B cells (*CD20*),

macrophages (CD68), and dendritic cells (CD11) in OC tissues, confirming the correlation between these three genes and immunity (Fig. 6, Supplementary Fig. 2).

3.7. Knockdown of *CDNS* exhibits tumor-suppressive effects in OC

Our results showed that *CDSN* was linked to a poor prognosis and involved immune infiltration in OC. We thus explored the function of *CDNS* in OC cells. We knocked down *CDNS* expression utilizing siRNAs in SKOV3 and HEY cells and verified down-regulation by Western blot and qRT-PCR (Fig. 7A-B , Supplementary Table 1). CCK-8 and colony formation assays suggested that the proliferation and colony formation rates were markedly lowered in the *CDSN* knockdown group relative to the control group (Fig. 7C and D). Meanwhile, elevated levels of *CDSN* could promote the growth of OC cells (Supplementary Fig. 3 , Supplementary Table 1). We

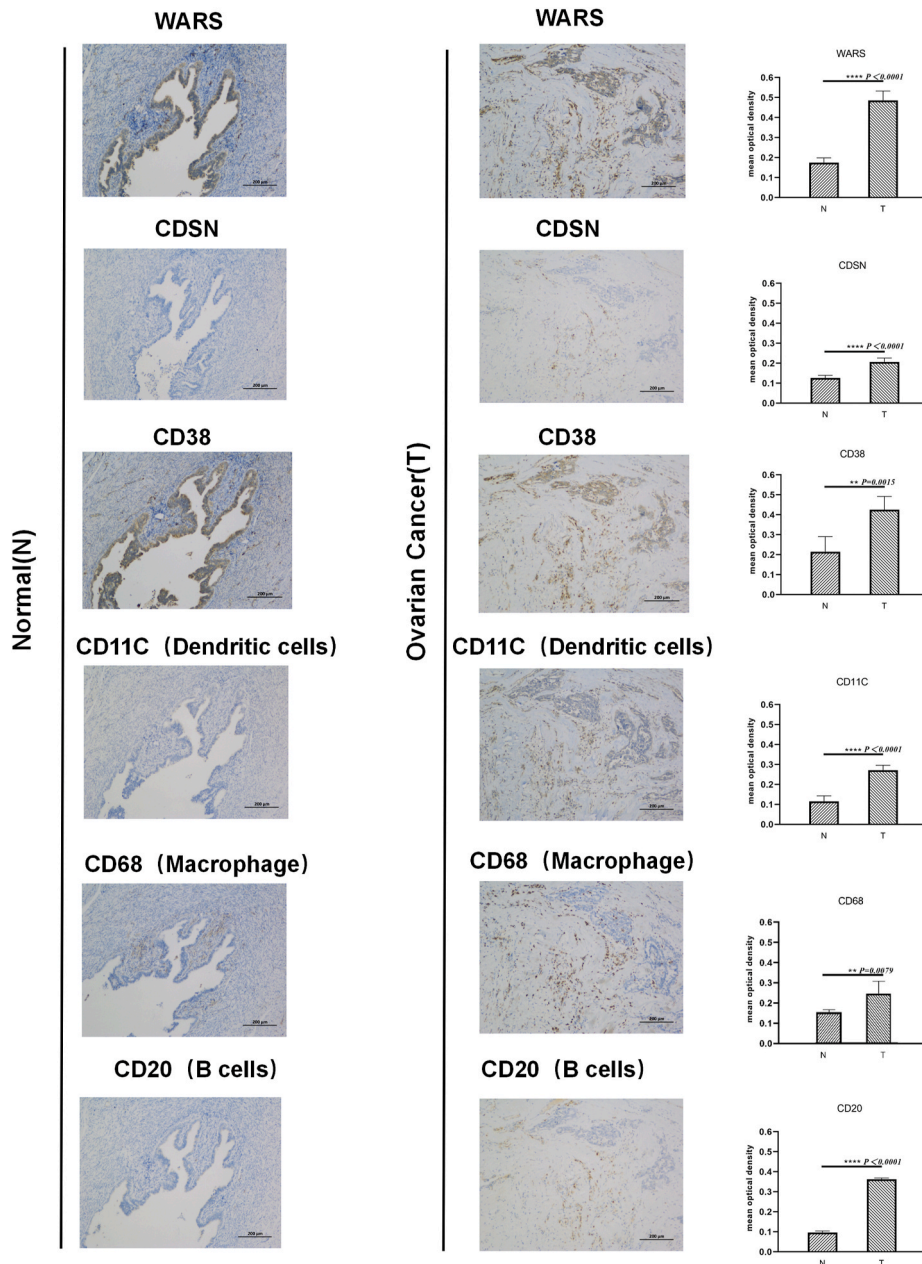
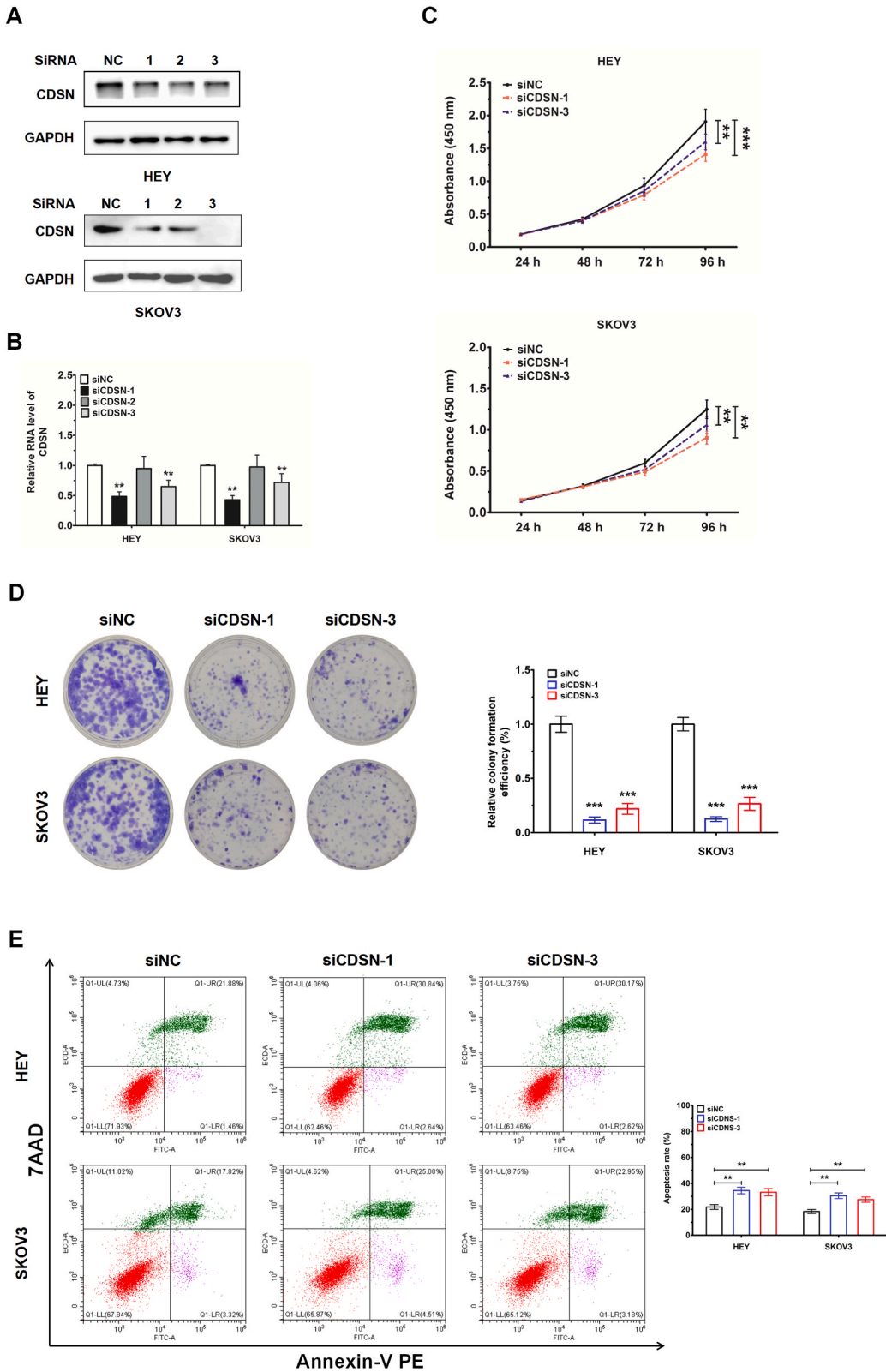


Fig. 6. Immuno-infiltration validation of candidate genes by IHC. Detection of WARS, CDSN, CD38, CD20, CD11C, and CD68 in normal ovarian tissue and the serous ovarian cancer tissue by IHC. The quantitative analysis of image by mean optical density (original magnification $\times 200$). Representative diagrams and quantification are shown. Bars represent SD from five random fields. All error bars = 95 % CIs. *P < 0.05, **P < 0.01, ***P < 0.001.



(caption on next page)

Fig. 7. The effect of knockdown of *CDSN* on OC cell proliferation. Examination of *CDSN* expression in *CDSN*-knockdown cells by (A) Western blot (B) qRT-PCR. (C) CCK-8 assay and (D) cell colony formation assay of proliferation of *CDSN*-knockdown cells. (E) Representative apoptotic profiles in cells with *CDSN* knockdown by flow cytometry. Representative diagrams and quantification are shown. Bars represent SD from three independent experiments. All error bars = 95 % CIs. * $P < 0.05$, ** $P < 0.01$, *** $P < 0.001$.

also evaluated the effects of *CDSN* knockdown on apoptosis using Annexin-V/PE and flow cytometry. The *CDSN* knockdown group exhibited a markedly elevated percentage of cell apoptosis (Fig. 7E). Specifically, the rates of apoptotic cells were 21.34 and 21.14 in HEY-siNC and SKOV3-siNC cells, but were 33.48 or 32.79 in si*CDSN*-treated HEY cells, and 29.51 or 26.13 in si*CDSN*-treated SKOV3 cells, respectively. The findings suggest that suppressing *CDSN* expression considerably diminished the growth and enhanced the apoptosis of OC cells.

4. Discussion

In the present study, bioinformatics analysis utilizing data from TCGA and GTEx databases suggested that *CDSN* was markedly associated with OC prognosis, tumor microenvironment, and mutations. This gene may represent a potential predictive biomarker for OC and thus may have value for clinical decision-making in the treatment and prognosis of OC.

The expression of three candidate genes (*CDSN*, *WARS*, and *CD38*) was observed to be markedly elevated in OC relative to normal tissues. *CDSN* is situated in the major histocompatibility complex class I region on chromosome 6 and encodes a protein found in keratodesmosomes, which are located in hair follicles and cornified epithelia [12,13]. *CDSN* functions as a cell-to-cell adhesion molecule [14]. In oral squamous cell carcinoma, low *CDSN* expression may be involved in cancer progression by contributing to oral inflammation, and individuals with decreased *CDSN* expression tend to have an unfavorable prognosis and short survival [15]. This is in contrast to our studies, and the difference may be attributable to different cancer types, cell types, and tumor microenvironments. *CDSN* is also intimately linked to inflammation. Research has demonstrated that dermatitis, a prevalent inflammatory manifestation of dermatitis syndrome, is attributed to autosomal recessive nonsense mutations in the *CDSN* gene [15]. Therefore, *CDSN* might be implicated in various forms of inflammation, which is crucial in the onset, progression, malignant transformation, invasion, metastasis, and other phases of cancer development. Nevertheless, the association between *CDSN* and OC has yet to be fully elucidated. Additionally, we explored the expression of *CDSN* in 33 different cancers. The findings suggested that *CDSN* was highly overexpressed in the majority of cancers, implying that *CDSN* may be an oncogene (Supplementary Fig. 4A). We also analyzed the correlation of *CDSN* with immune cells in different cancers. The results suggested that in most tumors, we observe that *CDSN* is associated with multiple infiltrating immune cells (Supplementary Fig. 4B). We further investigated the signaling pathways associated with *CDSN* in different tumors by gene set enrichment analysis (GSEA). The findings suggested that *CDSN* was markedly linked to the cancer-producing pathway in most cancers. For example, TNFA signaling via the NF- κ B pathway, KRAS signaling pathway, Inflammatory response, IL6-JAK-STAT3 signaling pathway, and P53 signaling pathway were enriched in the high *CDSN* group, suggesting that *CDSN* was positively correlated with these oncogenic pathways (Supplementary Fig. 4C). These pan-cancer analyses suggest that *CDSN* plays the role of a cancer-promoting factor in multi-tumors.

WARS encodes a tryptophanyl-tRNA synthetase consisting of 471 amino acids [16,17]. *WARS* is involved in protein synthesis and the pathophysiology of cancer and other diseases [18]. Studies have shown that the expression of *WARS* is elevated in uveal melanoma, oral squamous cell carcinoma, and cervical cancer, suggesting that *WARS* plays a crucial role in tumor initiation and progression [17, 19,20]. Furthermore, *WARS* may be a potential predictor of chemotherapy response in patients with hormone receptor-positive breast cancer [21]. High *WARS* expression has been associated with a good prognosis in microsatellite instability-type gastric cancer and poor prognosis in other gastric cancer types [22]. Our results suggest that high *WARS* expression is linked to good prognosis and positively correlated with immune infiltration in OC.

CD38 encodes for a 45 kDa single-chain type II transmembrane protein that are essential in mediating activation and proliferation signals across various immune cell [23]. Changes in *CD38* expression have been observed in multiple myeloma, natural killer cell lymphoma, and CD19 B-cell malignancies, and anti-*CD38* therapy has been confirmed as an effective treatment for a variety of hematologic malignancies and diseases [24]. *CD38* has also been shown to be both pro- and anti-tumorigenic in liver cancer, non-small-cell lung cancer, melanoma, pancreatic cancer, keratoma, and breast cancer. *CD38* was shown to be positively associated with OC prognosis and immune cell infiltration in the tumor microenvironment [25], aligning with the findings presented in this study.

The main studied immune checkpoint target in OC is the programmed death protein-1 (PD-1)/programmed death-ligand 1 (PD-L1) pathway [26]. OC expresses both PD-L2 and PD-L1, and dual inhibition of these targets is more effective than inhibiting each in isolation [27]. *CD38* is associated with PD-1/PD-L1, and co-treatment utilizing anti-*CD38* and PD-1/PD-L1 markedly reduced primary tumor growth in lung cancer by inhibiting acquired resistance to an immune checkpoint blockade, thereby improving and extending the effectiveness of anti-PD-1/PD-L1 [28]. Therefore, *CD38* may represent a potential therapeutic target in OC, and combination therapy with PD-1 inhibition may result in more effective treatment.

Our study has several limitations. First, our results lack validation in clinical sample tissues and clinical data or other datasets to verify the expression of genes in tissues and their correlation with patient prognosis and treatment. Second, there are significant clinical and molecular differences among different types of OC, and the potential impact of classification differences in OC on our results cannot be ruled out. Finally, there was an imbalance in sample disposition in the bioinformatics analysis of our study, with fewer normal samples than OC samples analyzed, which may have resulted in statistical bias.

Immunotherapy for OC has been less successful relative to most other immunogenic tumors, including non-small-cell lung cancer

and melanoma [29]. This may be attributable to the highly immunosuppressive effect of the tumor microenvironment in OC, which allows tumor cells to evade immune surveillance and achieve tumor proliferation [30]. Therefore, multiple biomarkers may be required to accurately predict treatment response. The results of the immune infiltration analysis suggested that WARS and CD38 were positively linked to immune cells such as T cells and antigen-presenting cells, and thus WARS and CD38 may represent potential biomarkers and therapeutic targets that maximize therapeutic benefits in patients with OC.

5. Conclusion

The present study has identified that the candidate gene *CDSN* exhibits high expression levels in OC and is closely correlated with immune infiltration and regulation. In vitro experimental validation demonstrated that inhibition of *CDSN* expression effectively suppresses OC cell proliferation. These findings suggest that *CDSN* holds promise as a potential diagnostic and prognostic marker, as well as a therapeutic target.

Funding

This study received support from the Yangfan Plan of Shanghai Science and Technology Commission (Grant No. 22YF1404700 for Ji) and the Research Start-up Fund of Huashan Hospital (Grant No. 2021QD043 for Ji).

Ethic statement

The research protocol underwent review and approval by the Ethics Committee of Fudan University Huashan Hospital (No. 2022-642), and informed consent was obtained from all study participants in accordance with institutional guidelines.

CRedit authorship contribution statement

Huan Zeng: Writing – original draft. **Wei Pan:** Methodology, Investigation. **Qiuyi Xia:** Resources, Data curation. **Hong Shu:** Supervision, Resources. **Zhaodong Ji:** Writing – review & editing, Funding acquisition.

Declaration of competing interest

The authors declare that they have no known competing financial interests or personal relationships that could have appeared to influence the work reported in this paper.

Abbreviations

Ovarian cancer OC
 Biological process BP
 Cellular component CC
 Copy number variations CNVs
 Corneodesmosin CDSN
 Progression-free survival PFS
 Gene Expression Profiling Interactive Analysis GEPIA
 Gene Ontology GO
 Genotype-tissue expression GTEx
 Kyoto Encyclopedia of Genes and Genomes KEGG
 Molecular functions MF
 Overall survival OS
 Ovarian cancer OC
 Programmed death protein-1 PD-1
 Programmed death-ligand 1 PD-L1
 Receiver operating characteristic ROC
 Tumor Immune Estimation ResourceTIMER

Appendix A. Supplementary data

Supplementary data to this article can be found online at <https://doi.org/10.1016/j.heliyon.2024.e33357>.

References

- [1] H. Sung, J. Ferlay, R.L. Siegel, M. Laversanne, I. Soerjomataram, A. Jemal, et al., Global cancer statistics 2020: GLOBOCAN estimates of incidence and mortality worldwide for 36 cancers in 185 countries, *CA Cancer J Clin* 713 (2021) 209–249.
- [2] J.A. Doherty, L.C. Peres, C. Wang, G.P. Way, C.S. Greene, J.M. Schildkraut, Challenges and opportunities in studying the epidemiology of ovarian cancer subtypes, *Curr Epidemiol Rep* 43 (2017) 211–220.
- [3] S.A. Gayther, P. Russell, P. Harrington, A.C. Antoniou, D.F. Easton, B.A. Ponder, The contribution of germline BRCA1 and BRCA2 mutations to familial ovarian cancer: no evidence for other ovarian cancer-susceptibility genes, *Am. J. Hum. Genet.* 654 (1999) 1021–1029.
- [4] U. Testa, E. Petrucci, L. Pasquini, G. Castelli, E. Pelosi, Ovarian cancers: genetic abnormalities, tumor heterogeneity and progression, clonal evolution and cancer stem cells, *Medicines (Basel)* 51 (2018).
- [5] H. Song, E. Dicks, S.J. Ramus, J.P. Tyrer, M.P. Interaggio, J. Hayward, et al., Contribution of germline mutations in the RAD51B, RAD51C, and RAD51D genes to ovarian cancer in the population, *J. Clin. Oncol.* 3326 (2015) 2901–2907.
- [6] S.J. Ramus, H. Song, E. Dicks, J.P. Tyrer, A.N. Rosenthal, M.P. Interaggio, et al., Germline mutations in the BRIP1, BARD1, PALB2, and NBN genes in women with ovarian cancer, *J. Natl. Cancer Inst.* 10711 (2015).
- [7] J.M. Hansen, R.L. Coleman, A.K. Sood, Targeting the tumour microenvironment in ovarian cancer, *Eur. J. Cancer* 56 (2016) 131–143.
- [8] R. Mandal, T.A. Chan, Personalized oncology meets immunology: the path toward precision immunotherapy, *Cancer Discov.* 67 (2016) 703–713.
- [9] K.A. Pankowska, G.E. Będkowska, J. Chociej-Stypuikowska, M. Rusak, M. Dąbrowska, J. Osada, Crosstalk of immune cells and platelets in an ovarian cancer microenvironment and their prognostic significance, *Int. J. Mol. Sci.* 2411 (2023).
- [10] H. Wang, M.M.H. Yung, H.Y.S. Ngan, K.K.L. Chan, D.W. Chan, The impact of the tumor microenvironment on macrophage polarization in cancer metastatic progression, *Int. J. Mol. Sci.* (2021) 2212.
- [11] C. Yang, B.R. Xia, Z.C. Zhang, Y.J. Zhang, G. Lou, W.L. Jin, Immunotherapy for ovarian cancer: adjuvant, combination, and neoadjuvant, *Front. Immunol.* 11 (2020) 577869.
- [12] N. Jonca, E.A. Leclerc, C. Caubet, M. Simon, M. Guerrin, G. Serre, Corneodesmosomes and corneodesmosin: from the stratum corneum cohesion to the pathophysiology of genodermatoses, *Eur. J. Dermatol.* 21 (Suppl 2) (2011) 35–42.
- [13] Y. Wu, B. Wang, J.L. Liu, X.H. Gao, H.D. Chen, Y.H. Li, Association of -619C/T polymorphism in CDSN gene and psoriasis risk: a meta-analysis, *Genet. Mol. Res.* 104 (2011) 3632–3640.
- [14] N. Jonca, M. Guerrin, K. Hadjiolova, C. Caubet, H. Gallinaro, M. Simon, et al., Corneodesmosin, a component of epidermal corneocyte desmosomes, displays homophilic adhesive properties, *J. Biol. Chem.* 2777 (2002) 5024–5029.
- [15] Y.B. Di, Y. Bao, J. Guo, W. Liu, S.X. Zhang, G.H. Zhang, et al., Corneodesmosin as a potential target of oral squamous cell carcinoma, *Medicine (Baltim.)* 10139 (2022) e28397.
- [16] F. Xu, G. Jiang, W. Li, X. He, Y. Jin, D. Wang, Three G.C base pairs required for the efficient aminoacylation of tRNA^{Trp} by tryptophanyl-tRNA synthetase from *Bacillus subtilis*, *Biochemistry* 4125 (2002) 8087–8092.
- [17] C.W. Lee, K.P. Chang, Y.Y. Chen, Y. Liang, C. Hsueh, J.S. Yu, et al., Overexpressed tryptophanyl-tRNA synthetase, an angiostatic protein, enhances oral cancer cell invasiveness, *Oncotarget* 626 (2015) 21979–21992.
- [18] Y.H. Ahn, S.C. Oh, S. Zhou, T.D. Kim, Tryptophanyl-tRNA synthetase as a potential therapeutic target, *Int. J. Mol. Sci.* (2021) 229.
- [19] P.P. Yang, X.H. Yu, J. Zhou, Tryptophanyl-tRNA synthetase (WARS) expression in uveal melanoma - possible contributor during uveal melanoma progression, *Biosci. Biotechnol. Biochem.* 843 (2020) 471–480.
- [20] H. Arnouk, M.A. Merkley, R.H. Podolsky, H. Stöppler, C. Santos, M. Alvarez, et al., Characterization of molecular markers indicative of cervical cancer progression, *Proteomics Clin. Appl.* 35 (2009) 516–527.
- [21] K.M. Lee, E.H. Hwang, S.E. Kang, C.H. Lee, H. Lee, H.J. Oh, et al., Tryptophanyl-tRNA synthetase sensitizes hormone receptor-positive breast cancer to docetaxel-based chemotherapy, *J. Breast Cancer* 236 (2020) 599–609.
- [22] S. Lu, L.J. Wang, K. Lombardo, Y. Kwak, W.H. Kim, M.B. Resnick, Expression of indoleamine 2, 3-dioxygenase 1 (Ido1) and tryptophanyl-tRNA synthetase (WARS) in gastric cancer molecular subtypes, *Appl. Immunohistochem. Mol. Morphol.* 285 (2020) 360–368.
- [23] M. Alessio, S. Roggero, A. Funaro, L.B. De Monte, L. Peruzzi, M. Geuna, et al., CD38 molecule: structural and biochemical analysis on human T lymphocytes, thymocytes, and plasma cells, *J. Immunol.* 1453 (1990) 878–884.
- [24] W. Szlasa, J. Czarny, N. Sauer, K. Rakoczy, N. Szymańska, J. Stecko, et al., Targeting CD38 in neoplasms and non-cancer diseases, *Cancers (Basel)* (2022) 1417.
- [25] Y. Zhu, Z. Zhang, Z. Jiang, Y. Liu, J. Zhou, CD38 predicts favorable prognosis by enhancing immune infiltration and antitumor immunity in the epithelial ovarian cancer microenvironment, *Front. Genet.* 11 (2020) 369.
- [26] G. Jiang, J. Hong, F. Shao, Q. Wen, F. Cheng, T. Yu, et al., Evolution of immunotherapy for ovarian cancer from a bird's-eye perspective: a text-mining analysis of publication trends and topics, *Front. Oncol.* 12 (2022) 795129.
- [27] Y.R. Miao, K.N. Thakkar, J. Qian, M.S. Kariolis, W. Huang, S. Nandagopal, et al., Neutralization of PD-L2 is essential for overcoming immune checkpoint blockade resistance in ovarian cancer, *Clin. Cancer Res.* 2715 (2021) 4435–4448.
- [28] L. Chen, L. Diao, Y. Yang, X. Yi, B.L. Rodriguez, Y. Li, et al., CD38-Mediated immunosuppression as a mechanism of tumor cell escape from PD-1/PD-L1 blockade, *Cancer Discov.* 89 (2018) 1156–1175.
- [29] S. Morand, M. Devanaboyina, H. Staats, L. Stanbery, J. Nemunaitis, Ovarian cancer immunotherapy and personalized medicine, *Int. J. Mol. Sci.* (2021) 2212.
- [30] K. Odunsi, Immunotherapy in ovarian cancer, *Ann. Oncol.* 28suppl_8 (2017) viii1–viii7.